
Score-Based Metropolis-Hastings Algorithms

Ahmed Aloui
Duke University

Ali Hasan
Morgan Stanley

Juncheng Dong
Duke University

Zihao Wu
Duke University

Vahid Tarokh
Duke University

Abstract

In this paper, we introduce a new approach for integrating score-based models with the Metropolis-Hastings algorithm. While traditional score-based diffusion models excel in accurately learning the score function from data points, they lack an energy function, making the Metropolis-Hastings adjustment step inaccessible. Consequently, the unadjusted Langevin algorithm is often used for sampling using estimated score functions. The lack of an energy function then prevents the application of the Metropolis-adjusted Langevin algorithm and other Metropolis-Hastings methods, limiting the wealth of other algorithms developed that use acceptance functions. We address this limitation by introducing a new loss function based on the *detailed balance condition*, allowing the estimation of the Metropolis-Hastings acceptance probabilities given a learned score function. We demonstrate the effectiveness of the proposed method for various scenarios, including sampling from heavy-tail distributions.

1 Introduction

Sampling from probability distributions with only access to samples is a longstanding problem with significant attention devoted to it in the statistics and machine learning communities (Goodfellow et al., 2020; Kingma, 2013; Ho et al., 2020; Dinh et al., 2016; Song et al., 2021). A wealth of literature and research is devoted to studying efficient methods for sampling from densities where only *a function proportional to the density* is known (Hastings, 1970; Wang et al.,

2024). A particular instance of this is the Metropolis-Hastings (MH) method, which provides a condition for accepting or rejecting new samples based on knowledge of the function proportional to the density (Robert et al., 2004). The MH algorithm builds a Markov chain based on a proposal distribution and an acceptance function and its convergence is guaranteed when the process satisfies the detailed balance condition. The success of this framework led to a significant amount of research effort devoted to algorithms that make use of the detailed balance criterion. Various MH algorithms have been introduced, defined by their choice of proposal distributions, such as the Random Walk Metropolis (RW) algorithm (Metropolis et al., 1953), the Metropolis Adjusted Langevin Algorithm (MALA) (Roberts and Tweedie, 1996; Roberts and Stramer, 2002), and the preconditioned Crank-Nicolson (pCN) algorithm (Hairer et al., 2014).

While these methods are theoretically well-grounded and provide strong empirical performance, they require knowledge of the unnormalized density, which may be difficult to obtain when only given samples. In recent years, score-based models have gained prominence due to their ability to learn the score function, i.e., the gradient of the log-density, directly from data samples (Song and Ermon, 2019; Song et al., 2020). Consequently, score-based sampling methods, such as the unadjusted Langevin algorithm, have primarily been employed to leverage the learned score function to sample from the target distribution (Grenander and Miller, 1994; Roberts and Tweedie, 1996).

With only knowledge of the score function, the research devoted to sampling using MH criteria is not used within the context of score-based generative modeling. This work proposes a unifying framework that bridges this gap, enabling the application of MH algorithms using only samples and a learned score function. Our analysis is motivated by two questions:

arXiv:2501.00467v1 [cs.LG] 31 Dec 2024

1. Can the acceptance function of an MH algorithm be estimated *solely based on the knowledge of an estimated score function*?
2. Does including an MH adjustment step *improve sample quality for score-based models*?

We answer these questions affirmatively by developing an approach to estimate an acceptance probability function from data and evaluating its effectiveness by comparing to ULA algorithms.

2 Related Work

A significant area of related work begins with estimating a score function for the data and then finding efficient ways of sampling using this estimated score function. While majority of such methods focus on designing sampling schemes that converge to the target distribution faster (e.g. through different numerical integrators), we consider our work as a parallel approach which uses an acceptance function to accept or reject different samples. This work lies at the intersection of the literature on score-based models and the Markov Chain Monte Carlo (MCMC) techniques that use Metropolis-Hastings acceptance functions. We then review recent works on score-based models and Metropolis-Hastings algorithms.

Score-Based Models. As mentioned within the introduction, many of the empirically successful sampling techniques involve sampling using an estimated score function (Song and Ermon, 2019; Song et al., 2021). These methods are trained using the score loss function by minimizing the Fisher divergence between the true and the predicted score (Hyvärinen, 2005; Vincent, 2011). A significant research effort is concerned with understanding the efficacy of these sampling algorithms, with some papers investigating the asymptotic error of score-based diffusion models, as in (Chen et al., 2023; Zhang et al., 2024). Different sampling schemes have been proposed to improve sampling speed and quality (Dockhorn et al., 2021; Lu et al., 2022; Chen et al., 2024). These methods have relied heavily on various score-based samplers such as ULA or the reverse-time SDE of a diffusion process (Song et al., 2021). Notably, Sjöberg et al. (2023) describe a line integration method to compute the acceptance probabilities.

Metropolis-Hastings Methods. Metropolis-Hastings (MH) algorithms are a class of MCMC algorithms that use an acceptance function to sample from target distributions (Metropolis et al., 1953; Hastings, 1970). These algorithms generate a se-

quence of samples by proposing a candidate state from a proposal distribution and accepting or rejecting the candidate based on an acceptance criterion that ensures convergence to the target distribution. The efficiency of MH algorithms heavily depends on the choice of the proposal distribution, and significant research effort has focused on designing efficient proposal mechanisms (Rosenthal et al., 2011; Song et al., 2017; Titsias and Dellaportas, 2019; Davies et al., 2023; Lew et al., 2023).

Recent developments in MH algorithms have explored the use of adaptive and state-dependent proposals to improve convergence rates and reduce autocorrelation in the generated samples (Andrieu and Thoms, 2008; Haario et al., 2001). These adaptive MH methods adjust the proposal distribution during the sampling process to better capture the geometry of the target distribution, leading to faster and more accurate sampling (Roberts and Rosenthal, 2009; Brooks et al., 2011; Hirt et al., 2021; Biron-Lattes et al., 2024).

3 Score-Based Metropolis-Hastings

Let $X \sim p$ be a random variable, with support $\text{supp}(X) = \mathcal{X} \subset \mathbb{R}^d$ and p be its probability density function. We assume that p is unknown, and only samples of X are observed. Denote these observed samples by $\{x^{(i)}\}_{i=1}^N$, where N is the number of observed samples.

The MH algorithm involves an *acceptance function* $a: \mathcal{X} \times \mathcal{X} \rightarrow [0, 1]$, which defines the probability $a(x', x)$ of transitioning from the current $x \in \mathcal{X}$ to a proposal $x' \in \mathcal{X}$. The common choice of the acceptance function is given by:

$$a(x', x) = \min \left\{ 1, \frac{p(x')q(x|x')}{p(x)q(x'|x)} \right\} \quad (1)$$

where $p(x)$ is the target distribution and $q(x|x')$ is the proposal distribution. The MH algorithm proceeds as follows:

- **Initialize:** Set $x_1 \in \mathcal{X}$, number of iterations T , and proposal distribution $q(x'|x)$.
- **For** $t = 1, \dots, T$:
 - Propose $x' \sim q(x'|x_t)$.
 - Compute $a(x', x_t)$ in (1) as the acceptance probability.
 - Draw $u \sim \text{Uniform}(0, 1)$. If $u \leq a(x', x_t)$, accept $x_{t+1} = x'$, otherwise set $x_{t+1} = x_t$.

Note that for computing $a(x', x_t)$ in (1), a function proportional to $p(x)$ is needed. On the other hand,

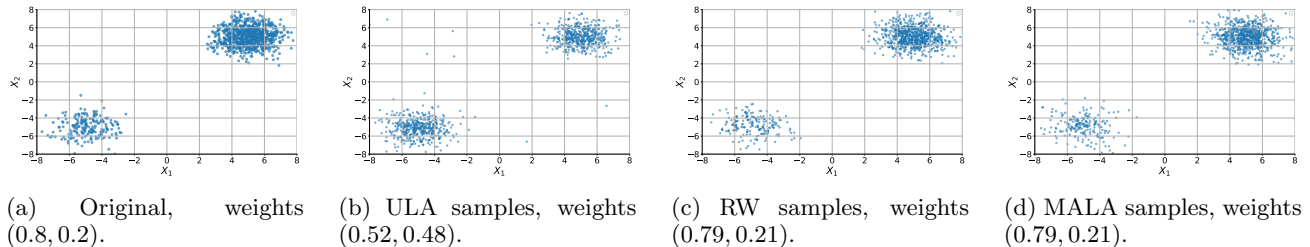


Figure 1: Comparison of sampling methods for a mixture of two Gaussians: (a) Original distribution, (b) ULA with the true scores, (c) RW with the true distribution, and (d) MALA with true scores and distribution. The plots demonstrate the impact of slow mixing between modes, highlighting the challenges in low-density regions. We report the empirical weights of the mixture given by each sampling method.

when sampling from $p(x)$, a common strategy is to estimate the score function $\nabla_x \log p(x)$ from data. In this work, we will assume that $\nabla_x \log p(x)$ is known through prior knowledge or estimated from the observed samples.

Detailed Balance. Although the acceptance function is often chosen according to (1), under mild conditions, the sufficient condition for convergence to the target distribution is that the acceptance ratio satisfies the *detailed balance* condition. The detailed balance condition, also known as the Markov reversibility condition, is defined as:

$$\forall x, x' \in \mathcal{X}, \quad \frac{a(x', x)}{a(x, x')} = \frac{p(x')q(x | x')}{p(x)q(x' | x)}. \quad (2)$$

Acceptance functions satisfying the detailed balance condition allow the Markov chain to have the target distribution as its unique stationary distribution under some mild assumptions. In particular, (1) is a particular solution to this condition. Our goal is then to use the knowledge of the stationary condition in (2) such that our sampling scheme is informed by this regime.

Balance Matching. To do this, we develop a loss function to *estimate a valid acceptance function from only the score function* based on the detailed balance condition given in (2). In the following proposition, we present the main observation motivating our method. We denote by ∇ the gradient with respect to $x, x' \in \mathbb{R}^d$, i.e., $\nabla = \nabla_{x, x'}$. Thus, for a function f with values in \mathbb{R} , the gradient ∇f has values in \mathbb{R}^{2d} .

Proposition 1. *If the gradients of the log acceptance ratio satisfy the following condition: for every $x, x' \in \mathcal{X}$,*

$$\nabla \log \left(\frac{a(x', x)}{a(x, x')} \right) = \nabla \log \left(\frac{p(x')}{p(x)} \right) + \nabla \log \left(\frac{q(x | x')}{q(x' | x)} \right) \quad (3)$$

then the acceptance function $a(x', x)$ must satisfy the

equality:

$$\frac{a(x, x')}{a(x', x)} = \frac{p(x')q(x | x')}{p(x)q(x' | x)}.$$

Proof. Proof is provided in appendix C. \square

It follows from Proposition 1 that matching the gradients of the left-hand side and right-hand side in (2) is a sufficient condition for verifying the detailed balance condition. In other words, if:

$$\begin{aligned} \nabla \log a(x', x) - \nabla \log a(x, x') \\ = \nabla \log p(x') - \nabla \log p(x) + \nabla \log q(x | x') \\ - \nabla \log q(x' | x), \end{aligned}$$

then the detailed balance condition is satisfied.

The acceptance function $a(x', x)$ can be modeled using an expressive class of functions, such as neural networks, and this function can be optimized to satisfy the condition in (3). In this setup, the gradients $\nabla \log a(x', x)$ and $\nabla \log a(x, x')$ correspond to the model's gradients, which can be efficiently computed via backpropagation when the model is differentiable. The terms $\nabla \log p(x)$ and $\nabla \log p(x')$ represent the score functions at x and x' , which can be approximated with a score model. We can express these score functions as:

$$\nabla \log p(x) = \nabla_{x, x'} \log p(x) = (\nabla_x \log p(x), \mathbf{0})^\top,$$

and, similarly,

$$\nabla \log p(x') = (\mathbf{0}, \nabla_{x'} \log p(x'))^\top,$$

where $\mathbf{0} \in \mathbb{R}^d$ is the zero vector. Finally, we note that the gradients of the proposal distribution $q(x'|x)$ are typically known by design when the proposal function is specified.

MH with an Estimated Acceptance Functions. In cases where the only a score function is available, we propose to estimate the acceptance function with balance matching using the estimated score

function so that MH algorithms can be applied. We term this approach *Score-Based Metropolis-Hastings*. For the scope of this paper, we will instantiate our method on three representative MH algorithms, specified by their proposal functions: the *Random Walk Metropolis-Hastings* (RW), the *Metropolis-Adjusted Langevin Algorithm* (MALA), and the *Preconditioned Crank-Nicolson* (pCN) algorithm. We next briefly review these methods.

Random Walk Metropolis-Hastings: In the RW algorithm, the proposal function is typically a Gaussian centered at the current state, i.e., $q(x' | x) = \mathcal{N}(x, \sigma^2 I)$, where σ^2 controls the step size of the random walk. This proposal is simple and symmetric, making it easy to implement.

Metropolis Adjusted Langevin Algorithm: MALA uses both the current state and the gradient of the log-probability. The proposal distribution is defined as $q(x' | x) = \mathcal{N}\left(x + \frac{\varepsilon^2}{2} \nabla \log p(x), \varepsilon^2 I\right)$, where ε is a step size parameter. This approach leverages the local gradient information to propose moves that are more likely to be accepted.

Preconditioned Crank-Nicolson: The pCN algorithm modifies the standard Crank-Nicolson approach by introducing a preconditioning step. The proposal function for pCN is given by $x' = \sqrt{1 - \beta^2} x + \beta \xi$, where $\xi \sim \mathcal{N}(0, I)$ is a standard Gaussian noise term and β controls the step size.

When the acceptance function is learned using balance matching, as defined in (3), we refer to these methods as **Score RW**, **Score MALA**, and **Score pCN**, respectively. While we illustrate our results on these three MH algorithms, we note that *the proposed framework is general* and can be applied to other proposal functions.

Slow Mixing. There are two main motivations for our approach. The first is the challenge of applying traditional MH algorithms to generative modeling without requiring knowledge of the unnormalized density, while assuming that the score function can be accurately learned. The second motivation arises from limitations of the unadjusted Langevin algorithm (ULA), which, although commonly used for sampling from score-based models, does not guarantee convergence to the true distribution due to the impact of discretization.

Consequently, by incorporating an MH adjustment step, we address a key limitation observed in the ULA when sampling from distributions with multiple modes, particularly when these modes are separated by regions of low density. Specifically, when the data distribution is a mixture $p(x) = \pi p_1(x) + (1 - \pi)p_2(x)$,

where $p_1(x)$ and $p_2(x)$ are distinct and largely disjoint distributions, the gradient of the log probability density, $\nabla_x \log p(x)$, becomes problematic. In regions where $p_1(x)$ dominates, the score is driven solely by $p_1(x)$, and similarly for $p_2(x)$. Consequently, ULA, which relies on these score gradients, fails to correctly sample from the mixture distribution as it does not properly account for the mixing proportions π and $1 - \pi$. This leads to an incorrect estimation of the relative densities between the modes. The faster mixing time of MALA compared to Langevin has been well-established in the literature as in (Dwivedi et al., 2019; Wu et al., 2022).

To illustrate this, we conduct experiments to generate a mixture of Gaussian distributions with $p_1 = \mathcal{N}((5, 5)^\top, I)$ and $p_2 = \mathcal{N}((-5, -5)^\top, I)$, with $\pi = 0.8$. As can be observed in Figure 1, ULA produces samples that *misrepresent the relative weights* of the modes. On the other hand, we observe that the original MH algorithms *significantly alleviate this problem*, generating samples with mode weights close to the truth. This leads to our Score-Based MH framework, which facilitates the application of MH algorithms when only score functions are available.

4 Algorithm

4.1 Acceptance Loss Function

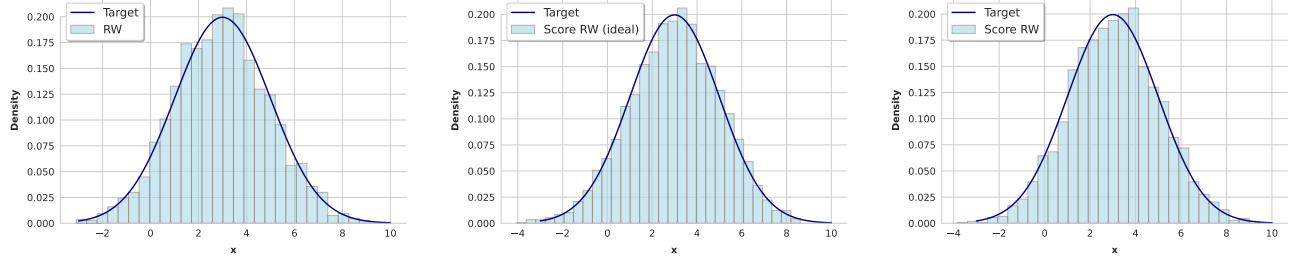
Ideal Acceptance Loss. We begin with the ideal scenario where the true score function $\nabla \log p$ is known. In this scenario, we propose the following loss function

$$\begin{aligned} \mathcal{L}_i(a) = \mathbb{E} \left[& \|\nabla \log a(X', X) - \nabla \log a(X, X') \right. \\ & - \nabla \log p(X') + \nabla \log p(X) \\ & \left. - \nabla \log q(X | X') + \nabla \log q(X' | X)\|^2 \right], \quad (4) \end{aligned}$$

with $X \sim p$ and $X' \sim q$, and the optimization objective is to learn an acceptance function $a^* \in \mathcal{F}$, where \mathcal{F} is a set of hypotheses, such that

$$a^* = \arg \min_{a \in \mathcal{F}} \mathcal{L}_i(a).$$

Practical Acceptance Loss. Typically, only samples from the data-generating process are observed, and the true $\nabla \log p$ is unknown. However, score parameterization through a neural network has proven successful in practice. We assume that we have an approximation of the score function previously estimated through a model $\tilde{s}(x) \approx \nabla \log p(x)$. Note that this is often the case in practice where an estimated



(a) Standard Random Walk Sampling. (b) Score-based RW with true scores. (c) Score-based RW with learned score.

Figure 2: Comparison of sampling methods from a Gaussian distribution $\mathcal{N}(3, 2)$ using three approaches: (a) Standard Random Walk Sampling with the acceptance function defined in (1), (b) Score-based RW with an acceptance network trained using true scores, and (c) Score-based RW with an acceptance network trained using a learned score.

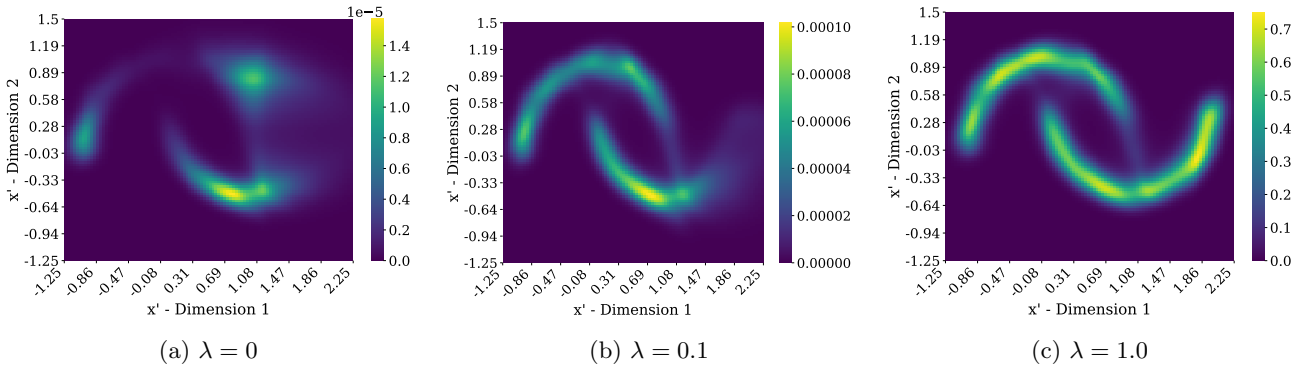
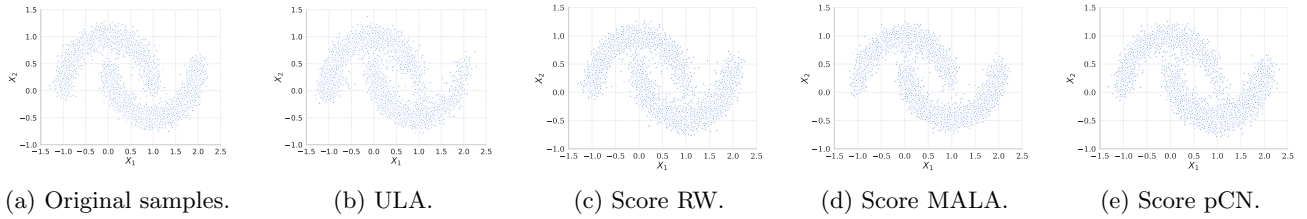
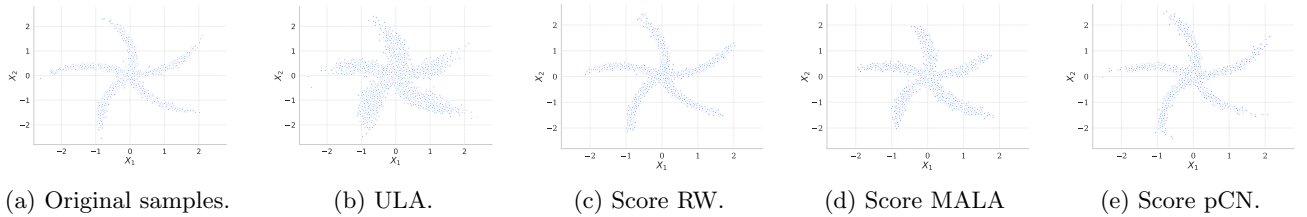


Figure 3: Visualizing the acceptance probabilities for different values of x' for a given initial state $x = (0.0, 0.0)$. We plot the results for training an acceptance network with three different regularization values $\lambda \in \{0, 0.1, 1.0\}$



(a) Original samples. (b) ULA. (c) Score RW. (d) Score MALA. (e) Score pCN.

Figure 4: Comparison of different methods on the Moons dataset.



(a) Original samples. (b) ULA. (c) Score RW. (d) Score MALA. (e) Score pCN.

Figure 5: Comparison of different methods on the Pinwheel dataset.

score function \tilde{s} is used in conjunction with ULA for sampling. In this scenario, the proposed practical loss

function is

$$\mathcal{L}_p(a) = \mathbb{E} \left[\|\nabla \log a(X', X) - \nabla \log a(X, X') - \tilde{s}(X') + \tilde{s}(X) - \nabla \log q(X | X') + \nabla \log q(X' | X)\|^2 \right], \quad (5)$$

with $X \sim p$ and $X' \sim q$, and the optimization objective is to learn an acceptance function $\tilde{a} \in \mathcal{F}$ where

$$\tilde{a} = \arg \min_{a \in \mathcal{F}} \mathcal{L}_p(a).$$

Illustrative Example. We present the sampling results from a Gaussian distribution $\mathcal{N}(3, 2)$ using the original Random Walk Metropolis-Hastings Algorithm, as shown in Figure 2a. Next, we show the results of training with the ideal loss function for the Score-based RW in Figure 2b, followed by the results using the practical loss function for Score-based RW in Figure 2c.

4.2 Entropy Regularization

Moreover, our algorithm involves an entropy regularization term alongside the proposed loss function defined in Section 4.1. To illustrate its effectiveness, we present the following result as motivation.

Proposition 2 (Estimated Acceptance Function). *Let $x, x' \in \mathcal{X}$, and let $M \geq 1$. Then, the acceptance function defined as:*

$$a_M(x', x) = \min \left\{ \frac{1}{M}, \frac{1}{M} \frac{p(x')q(x | x')}{p(x)q(x' | x)} \right\}$$

satisfies the detailed balance condition in (2).

Proof. Proof is provided in the appendix. \square

It follows from Proposition 2 that there are infinitely many solutions to the detailed balance condition, and the acceptance probabilities can become infinitesimally small. While each of these acceptance functions is a mathematically valid solution to the detailed balance condition, in practice, sampling with these low-acceptance probability functions can lead to always rejecting the proposal, resulting in a lack of convergence within a reasonable timeframe.

Therefore, if we *solely* optimize the loss functions in (4) and (5), we risk converging to minima that are legitimate solutions but impractical due to their very low acceptance probabilities. To address this issue, we propose adding an entropy regularization term to our loss function. The modified loss function is given by:

$$\begin{aligned} \mathcal{L}(a) = & \mathbb{E} \left[\left\| \nabla \log a(X', X) - \nabla \log a(X, X') \right. \right. \\ & - \tilde{s}(X') + \tilde{s}(X) - \nabla \log q(X | X') \\ & \left. \left. + \nabla \log q(X' | X) \right\|^2 \right] + \lambda \mathbb{E} [H(\log a(X', X))], \end{aligned} \quad (6)$$

where

$$\begin{aligned} H(a(X', X)) = & \log(a(X', X))a(X', X) \\ & + \log(1 - a(X', X))(1 - a(X', X)). \end{aligned}$$

and $\lambda \geq 0$ is the weight of the regularization term. This regularization term encourages acceptance functions with higher entropy acceptance probabilities, thereby avoiding minima that result in very low acceptance probabilities.

To illustrate the importance of the regularization term, we present the results using the Moons dataset from `scikit-learn` (Pedregosa et al., 2011). Based on an estimated score function, we estimate an acceptance function to sample from the Moons dataset using the proposed Score RW algorithm. Training is done for different values of the regularization parameter λ , and the results are plotted in Figure 3. It can be observed that the acceptance probability is significantly enhanced with the regularization whereas training without the entropy regularization results in acceptance probability close 0. Although this acceptance probability remains mathematically valid (i.e., it will still converge to the target distribution), the convergence time may become impractically long.

4.3 Implementation

The final loss function used to train the acceptance network in our score MH framework consists of two components: the primary loss term, which enforces the reversibility condition, and an entropy regularization term. The primary loss is designed to minimize the difference between the gradients of the log acceptance probability and the gradients of the log posterior and proposal distributions.

$$\mathcal{L}_{\text{emp}}(a) = \frac{1}{N} \sum_{i=1}^N l_i(a) + \frac{\lambda}{N} \sum_{i=1}^N h_i(a) \quad (7)$$

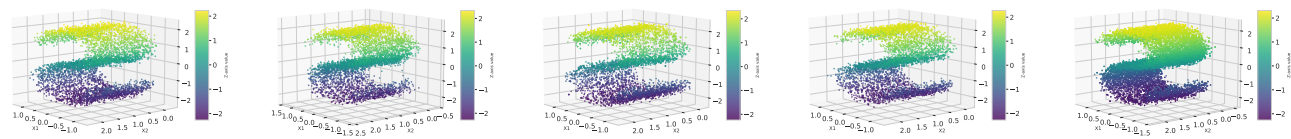
with

$$\begin{aligned} l_i(a) = & \left\| \nabla \log a(x'^{(i)}, x^{(i)}) - \nabla \log a(x^{(i)}, x'^{(i)}) \right. \\ & - \tilde{s}(x'^{(i)}) + \tilde{s}(x^{(i)}) \\ & \left. - \nabla \log q(x^{(i)} | x'^{(i)}) + \nabla \log q(x'^{(i)} | x^{(i)}) \right\|^2 \end{aligned}$$

and

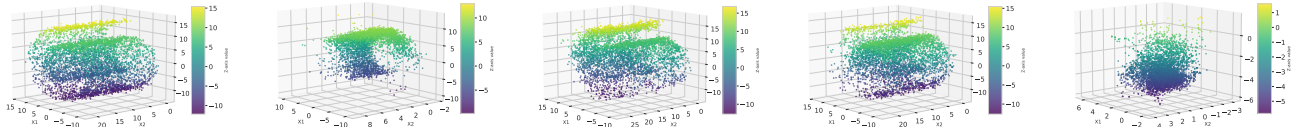
$$\begin{aligned} h_i(a) = & \log a(x'^{(i)}, x^{(i)}) \cdot a(x'^{(i)}, x^{(i)}) \\ & + \log(1 - a(x'^{(i)}, x^{(i)})) \cdot (1 - a(x'^{(i)}, x^{(i)})). \end{aligned}$$

and where $x'^{(i)} = \alpha v' + (1 - \alpha)\tilde{x}$, with $\tilde{x} \sim p$ and $v' \sim q(\cdot | \tilde{x})$, where $\alpha \in [0, 1]$ controls how much x'



(a) Original samples. (b) ULA. (c) Score RW. (d) Score MALA. (e) Score pCN.

Figure 6: Comparison of different methods on the S-curve dataset.



(a) Original samples. (b) ULA. (c) Score RW. (d) Score MALA. (e) Score pCN.

Figure 7: Comparison of different methods on the Swiss Roll dataset.

deviates from the data distribution towards the proposal. In the first epochs of training, we begin with smaller values of α to favor data from the true distribution, and then gradually increase α to estimate the acceptance function around the proposal region. This approach is motivated by the fact that the score function may not be well-estimated outside of the data region, and starting with smaller α helps prevent biasing the training with poorly learned scores.

We present the pseudo-code for the proposed loss function in Algorithm 1 and the training procedure in Algorithm 2. We made several design choices that we observed to be beneficial for learning stable acceptance probabilities:

- Using residual blocks akin to He et al. (2016).
- Employing smooth activation functions, such as GeLU or Softplus.
- Implementing annealed sampling from the proposal distribution, where instead of directly sampling from the target distribution, we start from a weighted combination of the observed data samples and the proposal samples.

5 Empirical Results

In this section, we present the empirical results on benchmark datasets including (Moons, Pinwheel, S-curve, and Swiss Roll), to demonstrate the validity of our approach. The results are presented in Figures 4, 5, 6, and 7.

Algorithm 1 Acceptance Loss Function

Input: Acceptance net $a(x', x)$, Score Net s , batch of samples b_x , batch of proposals $b_{x'}$, regularization parameter λ , gradient clipping threshold C .

Step 1: Compute gradients $\nabla \log a(x', x)$ and $\nabla \log a(x, x')$ using Autograd for every $(x, x') \in b_x \times b_{x'}$.

Step 2: Compute score gradients $s(x)$ and $s(x')$ for every $(x, x') \in b_x \times b_{x'}$.

Step 3: Compute proposal gradients $\nabla q(x|x')$ and $\nabla q(x'|x)$ for every $(x, x') \in b_x \times b_{x'}$.

Step 4: Clip all gradients to avoid instability using threshold C .

Step 5: Compute the loss \mathcal{L}_{emp} as defined in (7).

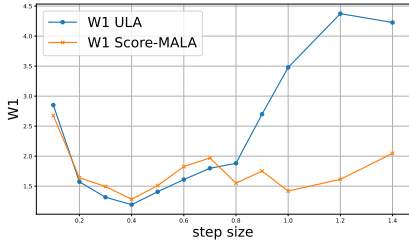
Output: \mathcal{L}_{emp}

Results Analysis. The results in Table 1 illustrate the performance of four sampling methods: ULA, Score-based RW, Score-based MALA, and Score-based pCN, across four datasets using three evaluation metrics: Wasserstein-1 (W1), Wasserstein-2 (W2), and Maximum Mean Discrepancy (MMD).

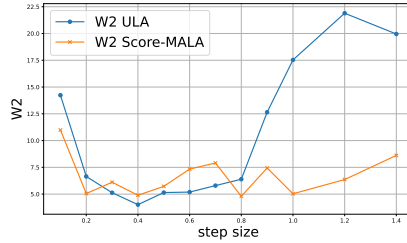
Overall, the Score RW method consistently achieves lower W1 and W2 values compared to ULA across all datasets, highlighting its efficiency in sample-based inference. This trend is especially noticeable on the Moons and Pinwheel datasets, where the W2 metric significantly outperforms that of the ULA method. For more complex datasets like Swiss Roll, the score MH algorithms show noticeable improvements, with Score RW and Score MALA achieving significantly lower W1

Table 1: Quantitative comparison of methods across the datasets using the following metrics: Wasserstein-1 (W1), Wasserstein-2 (W2), and Maximum Mean Discrepancy (MMD).

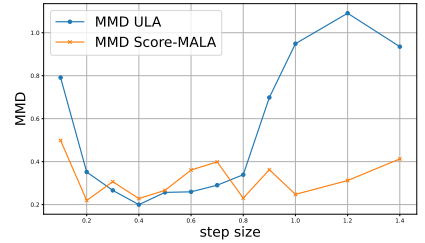
Dataset	ULA			Score RW			Score MALA			Score pCN		
Metric	W1	W2	MMD	W1	W2	MMD	W1	W2	MMD	W1	W2	MMD
Moons	0.143	0.096	0.054	0.019	0.007	0.004	0.018	0.004	0.002	0.039	0.021	0.012
Pinwheel	0.106	0.062	0.022	0.012	0.001	0.001	0.086	0.064	0.027	0.016	0.007	0.003
S-curve	0.082	0.055	0.016	0.050	0.015	0.004	0.046	0.014	0.004	0.090	0.051	0.017
Swiss Roll	2.881	14.409	0.811	2.270	8.470	0.400	1.399	4.575	0.245	14.167	113.824	6.903



(a) W1 vs step size



(b) W2 vs step size



(c) MMD vs step size

Figure 8: Influence of step size on the performance of Score-based MALA vs. ULA, evaluated on the Swiss Roll dataset.

Algorithm 2 Training the Acceptance Network

Input: Acceptance Network a , Score Network s , dataset D , number of epochs N , sequence $\{\alpha_i\}_{i=1}^N \subset [0, 1]$ (increasing).

For each epoch $i = 1$ to N :

1. Sample a batch b_x and a batch $b_{\tilde{x}}$ from D .
2. For each $\tilde{x} \in b_{\tilde{x}}$, sample $v' \sim q(\cdot | \tilde{x})$ and set $x' = \alpha_i v' + (1 - \alpha_i)\tilde{x}$.
3. Compute the loss as defined in Algorithm 1.
4. Update the Acceptance Network a using the Adam optimizer.

Output: Trained Acceptance Network a .

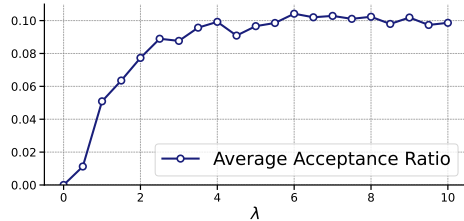


Figure 9: Average acceptance ratio as a function of λ . The average acceptance ratio is calculated by evaluating the acceptance network over a uniform grid of x' values, with ranges $[-1.5, 2.25]$ for the first dimension and $[-1, 1.5]$ for the second dimension, while keeping $x = (0, 0)$ fixed. The mean acceptance ratio is then obtained by averaging uniformly over the grid.

and MMD scores when compared to the other methods.

Stability with respect to Step Size: Score MALA vs. ULA. The results demonstrate that Score MALA is more robust to variations in step size compared to ULA. As seen in Figure 8, the W1, W2, and MMD metrics consistently show lower sensitivity to changes in step size for Score MALA, indicating its stability across different settings.

Effect of Entropy Regularization. We study the effect of the entropy regularization term on the Moons

dataset. As shown in Figure 9, the relationship between the entropy regularization parameter λ and the average acceptance ratio indicates a significant impact on the sampling efficiency. As λ increases from 0 to around 4, the average acceptance ratio rises sharply, suggesting that stronger entropy regularization enhances learning more practical acceptance functions. Beyond $\lambda = 4$, the acceptance ratio plateaus. This demonstrates that the performance remains robust for larger values of the entropy regularization term.

6 Discussion

In this work we describe a method for estimating the acceptance function given only knowledge of samples and an estimated score function. We demonstrated the successful estimation of an acceptance function applicable across various MH sampling algorithms. While we empirically evaluate on three particular instances, this work opens the door for further implementations and techniques for sampling using acceptance functions. Additionally, we discussed a particular class of acceptance functions that are amenable for efficient sampling using entropy regularization. The proposed methods provide new avenues for combining MH within the context of score-based generative modeling.

Limitations. The main limitation of the method is the additional computational cost required to train the acceptance network. Furthermore, more advanced architectures need to be proposed to extend this framework to high-dimensional data. Additionally, further theoretical analysis is needed to provide more appropriate priors on which acceptance function should be chosen.

Acknowledgments Vahid Tarokh’s work was supported in part by the Air Force Office of Scientific Research under award number FA9550-20-1-0397.

References

- Christophe Andrieu and Johannes Thoms. A tutorial on adaptive mcmc. *Statistics and computing*, 18: 343–373, 2008.
- Miguel Biron-Lattes, Nikola Surjanovic, Saifuddin Syed, Trevor Campbell, and Alexandre Bouchard-Côté. automala: Locally adaptive metropolis-adjusted langevin algorithm. In *International Conference on Artificial Intelligence and Statistics*, pages 4600–4608. PMLR, 2024.
- Steve Brooks, Andrew Gelman, Galin Jones, and Xiao-Li Meng. *Handbook of markov chain monte carlo*. CRC press, 2011.
- Sitan Chen, Sinho Chewi, Jerry Li, Yuanzhi Li, Adil Salim, and Anru Zhang. Sampling is as easy as learning the score: theory for diffusion models with minimal data assumptions. In *The Eleventh International Conference on Learning Representations*, 2023.
- Yuzhu Chen, Fengxiang He, Shi Fu, Xinmei Tian, and Dacheng Tao. Adaptive time-stepping schedules for diffusion models. In *The 40th Conference on Uncertainty in Artificial Intelligence*, 2024.
- Laurence Davies, Robert Salomone, Matthew Sutton, and Chris Drovandi. Transport reversible jump proposals. In Francisco Ruiz, Jennifer Dy, and Jan-Willem van de Meent, editors, *Proceedings of The 26th International Conference on Artificial Intelligence and Statistics*, volume 206 of *Proceedings of Machine Learning Research*, pages 6839–6852. PMLR, 25–27 Apr 2023.
- Laurent Dinh, Jascha Sohl-Dickstein, and Samy Bengio. Density estimation using real nvp. *arXiv preprint arXiv:1605.08803*, 2016.
- Tim Dockhorn, Arash Vahdat, and Karsten Kreis. Score-based generative modeling with critically-damped langevin diffusion. *arXiv preprint arXiv:2112.07068*, 2021.
- Raaz Dwivedi, Yuansi Chen, Martin J Wainwright, and Bin Yu. Log-concave sampling: Metropolis-hastings algorithms are fast. *Journal of Machine Learning Research*, 20(183):1–42, 2019.
- Ian Goodfellow, Jean Pouget-Abadie, Mehdi Mirza, Bing Xu, David Warde-Farley, Sherjil Ozair, Aaron Courville, and Yoshua Bengio. Generative adversarial networks. *Communications of the ACM*, 63(11): 139–144, 2020.
- Ulf Grenander and Michael I Miller. Representations of knowledge in complex systems. *Journal of the Royal Statistical Society: Series B (Methodological)*, 56(4):549–581, 1994.
- Heikki Haario, Eero Saksman, and Johanna Tamminen. An adaptive metropolis algorithm. *Bernoulli*, 7(2):223–242, April 2001.
- Martin Hairer, Andrew M. Stuart, and Sebastian J. Vollmer. Spectral gaps for a metropolis-hastings algorithm in infinite dimensions. *The Annals of Applied Probability*, 24(6):2455–2490, December 2014.
- W. Keith Hastings. Monte carlo sampling methods using markov chains and their applications. *Biometrika*, 1970.
- Kaiming He, Xiangyu Zhang, Shaoqing Ren, and Jian Sun. Deep residual learning for image recognition. In *Proceedings of the IEEE conference on computer vision and pattern recognition*, pages 770–778, 2016.
- Marcel Hirt, Michalis Titsias, and Petros Dellaportas. Entropy-based adaptive hamiltonian monte carlo. *Advances in Neural Information Processing Systems*, 34:28482–28495, 2021.
- Jonathan Ho, Ajay Jain, and Pieter Abbeel. Denoising diffusion probabilistic models. *Advances in neural information processing systems*, 33:6840–6851, 2020.
- Aapo Hyvärinen. Estimation of non-normalized statistical models by score matching. *Journal of Machine Learning Research*, 6(4), 2005.
- Diederik P Kingma. Auto-encoding variational bayes. *arXiv preprint arXiv:1312.6114*, 2013.

- Alexander K. Lew, George Matheos, Tan Zhi-Xuan, Matin Ghavamizadeh, Nishad Gothoskar, Stuart Russell, and Vikash K. Mansinghka. Smcp3: Sequential monte carlo with probabilistic program proposals. In *Proceedings of The 26th International Conference on Artificial Intelligence and Statistics*, pages 7061–7088, 2023.
- Cheng Lu, Yuhao Zhou, Fan Bao, Jianfei Chen, Chongxuan Li, and Jun Zhu. Dpm-solver: A fast ode solver for diffusion probabilistic model sampling in around 10 steps. *Advances in Neural Information Processing Systems*, 35:5775–5787, 2022.
- Nicholas Metropolis, Arianna W Rosenbluth, Marshall N Rosenbluth, Augusta H Teller, and Edward Teller. Equation of state calculations by fast computing machines. *The journal of chemical physics*, 21(6):1087–1092, 1953.
- F. Pedregosa, G. Varoquaux, A. Gramfort, V. Michel, B. Thirion, O. Grisel, M. Blondel, P. Prettenhofer, R. Weiss, V. Dubourg, J. Vanderplas, A. Passos, D. Cournapeau, M. Brucher, M. Perrot, and E. Duchesnay. Scikit-learn: Machine learning in Python. *Journal of Machine Learning Research*, 12: 2825–2830, 2011.
- Christian P Robert, George Casella, Christian P Robert, and George Casella. The metropolis—hastings algorithm. *Monte Carlo statistical methods*, pages 267–320, 2004.
- Gareth O Roberts and Jeffrey S Rosenthal. Examples of adaptive mcmc. *Journal of computational and graphical statistics*, 18(2):349–367, 2009.
- Gareth O Roberts and Osnat Stramer. Langevin diffusions and metropolis-hastings algorithms. *Methodology and computing in applied probability*, 4:337–357, 2002.
- Gareth O. Roberts and Richard L. Tweedie. Exponential convergence of langevin distributions and their discrete approximations. *Bernoulli*, 2(4):341–363, December 1996.
- Jeffrey S Rosenthal et al. Optimal proposal distributions and adaptive mcmc. *Handbook of Markov Chain Monte Carlo*, 4(10.1201), 2011.
- Anders Sjöberg, Jakob Lindqvist, Magnus Önnheim, Mats Jirstrand, and Lennart Svensson. Mcmc-correction of score-based diffusion models for model composition. *arXiv preprint arXiv:2307.14012*, 2023.
- Jiaming Song, Shengjia Zhao, and Stefano Ermon. Anice-mc: Adversarial training for mcmc. *Advances in neural information processing systems*, 30, 2017.
- Yang Song and Stefano Ermon. Generative modeling by estimating gradients of the data distribution. *Advances in neural information processing systems*, 32, 2019.
- Yang Song, Sahaj Garg, Jiaxin Shi, and Stefano Ermon. Sliced score matching: A scalable approach to density and score estimation. In *Uncertainty in Artificial Intelligence*, pages 574–584. PMLR, 2020.
- Yang Song, Jascha Sohl-Dickstein, Diederik P Kingma, Abhishek Kumar, Stefano Ermon, and Ben Poole. Score-based generative modeling through stochastic differential equations. In *International Conference on Learning Representations*, 2021.
- Michalis Titsias and Petros Dellaportas. Gradient-based adaptive markov chain monte carlo. *Advances in neural information processing systems*, 32, 2019.
- Pascal Vincent. A connection between score matching and denoising autoencoders. *Neural computation*, 23(7):1661–1674, 2011.
- Liwei Wang, Xinru Liu, Aaron Smith, and Aguemon Y Atchade. On cyclical mcmc sampling. In *International Conference on Artificial Intelligence and Statistics*, pages 3817–3825. PMLR, 2024.
- Keru Wu, Scott Schmidler, and Yuansi Chen. Minimax mixing time of the metropolis-adjusted langevin algorithm for log-concave sampling. *Journal of Machine Learning Research*, 23(270):1–63, 2022.
- Kaihong Zhang, Heqi Yin, Feng Liang, and Jingbo Liu. Minimax optimality of score-based diffusion models: Beyond the density lower bound assumptions. In *Proceedings of the 41st International Conference on Machine Learning*, volume 235 of *Proceedings of Machine Learning Research*, pages 60134–60178. PMLR, 21–27 Jul 2024.

Appendix

In this appendix, we first discuss an alternative approximation of the acceptance function that relies solely on the score functions, derived using the Taylor expansion of the log densities. Next, we consider sampling with score-based MALA for heavy-tailed distributions. Third, we provide the proofs for the theoretical results. Finally, we present additional details of the experiments.

A Taylor Score-based Metropolis-Hastings

In this section, we propose an approximation of the acceptance function based on the Taylor expansion of the log densities.

For an acceptance function $a(x'|x)$ as defined in Equation 1, the ratio $r(x', x) = \frac{p(x')q(x|x')}{p(x)q(x'|x)}$ can be rewritten as:

$$\log(r(x', x)) = \log p(x') - \log p(x) + \log q(x | x') - \log q(x' | x) \quad (8)$$

Let $\tau = x' - x$. Assuming that $\|\tau\|$ is sufficiently small, we perform a second-order Taylor series expansion of the logarithmic terms around the point x .

Taylor Expansion of $\log p(x')$ Around x : Expanding $\log p(x') = \log p(x + \tau)$ using a second-order Taylor series:

$$\log p(x + \tau) = \log p(x) + \nabla \log p(x) \cdot \tau + \frac{1}{2} \tau^\top \nabla^2 \log p(x) \tau + o(\|\tau\|^2) \quad (9)$$

Therefore,

$$\log p(x') - \log p(x) = \nabla \log p(x) \cdot \tau + \frac{1}{2} \tau^\top \nabla^2 \log p(x) \tau + o(\|\tau\|^2) \quad (10)$$

Taylor Expansion of $\log p(x)$ Around x' : Similarly, expanding $\log p(x) = \log p(x' - \tau)$:

$$\log p(x' - \tau) = \log p(x') - \nabla \log p(x') \cdot \tau + \frac{1}{2} \tau^\top \nabla^2 \log p(x') \tau + o(\|\tau\|^2) \quad (11)$$

Rearranging gives:

$$\log p(x) - \log p(x') = -\nabla \log p(x') \cdot \tau + \frac{1}{2} \tau^\top \nabla^2 \log p(x') \tau + o(\|\tau\|^2) \quad (12)$$

Final Result Therefore, we have that,

$$\begin{aligned} \log p(x') - \log p(x) &= \frac{1}{2} (\log p(x') - \log p(x)) + \frac{1}{2} (\log p(x') - \log p(x)) \\ &= \frac{1}{2} [\nabla \log p(x) \cdot \tau + \nabla \log p(x') \cdot \tau] \\ &\quad + \frac{1}{4} \tau^\top (\nabla^2 \log p(x) - \nabla^2 \log p(x')) \tau + o(\|\tau\|^2) \end{aligned}$$

Simplifying, we obtain:

$$\log p(x') - \log p(x) = \frac{1}{2} (\nabla \log p(x) + \nabla \log p(x')) \cdot \tau + \frac{1}{4} \tau^\top (\nabla^2 \log p(x) - \nabla^2 \log p(x')) \tau + o(\|\tau\|^2) \quad (13)$$

Combining the above results, we have:

$$\log r(x', x) = \frac{1}{2} (\nabla \log p(x) + \nabla \log p(x')) \cdot \tau + \frac{1}{4} \tau^\top (\nabla^2 \log p(x) - \nabla^2 \log p(x')) \tau + o(\|\tau\|^2) + \log q(x | x') - \log q(x' | x)$$

If the distance between the Hessian is negligible, we can approximate the acceptance function as

$$\log r(x', x) \approx \frac{1}{2} (\nabla \log p(x) + \nabla \log p(x')) \cdot \tau + [\log q(x | x') - \log q(x' | x)]$$

We denote this approximation of the acceptance function as Taylor-1 (Averaging). Figure 10 illustrates how this approximation can provide a better result compared to the first-order and second-order Taylor series from Equation 10, while achieving very similar performance to the original Equation 13, which utilizes the Hessian terms. This is particularly important because computing the Hessian numerically (by backpropagation through a score model) is computationally expensive and unstable.

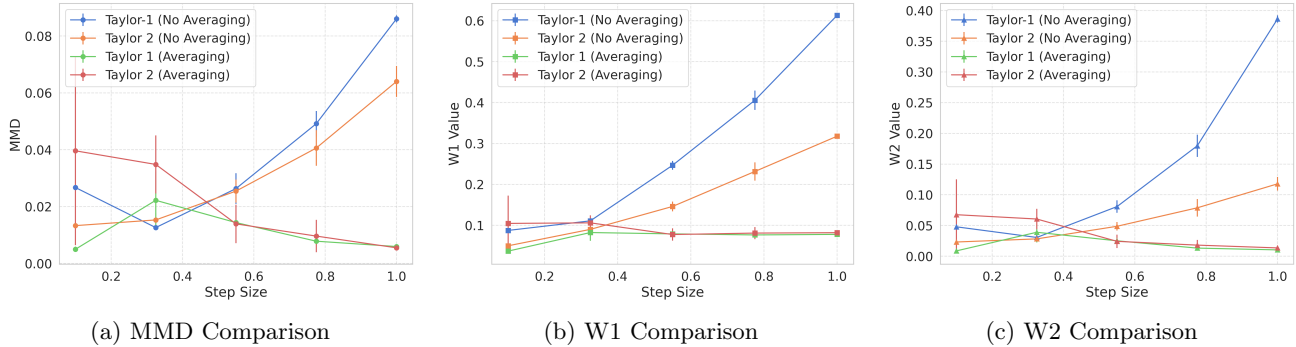


Figure 10: Comparison of Taylor approximations: Taylor-1 and Taylor-2 methods (with and without averaging) evaluated using MMD, W1, and W2 metrics. The experiments were conducted on the Moons dataset.

Additionally, Figure 11 compare the performance of Taylor-1 (Averaging) to score-based Metropolis-Hastings. We can see that for some range the Taylor approximation provides a very good approximation of the Acceptance function as it yields good sampling quality. However, even though some robustness is observed score-based MALA still outperforms the Taylor approximation.

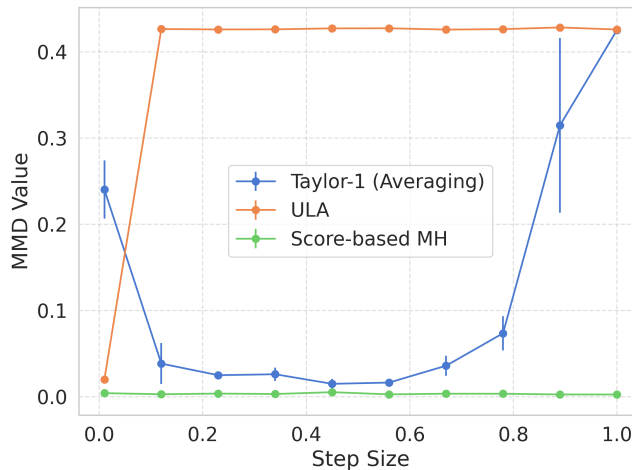


Figure 11: MMD distance comparison between ULA, Taylor-1 (Averaging), and Score-based MH.

B Metropolis-Hastings and Generalized Extreme Value Distributions

In this section, we study the effect of sampling using ULA, MALA, and score-based MALA algorithms. We analyze the impact of the adjustment step on distributions with heavy tails and hypothesize that as the tail becomes heavier, the adjustment step becomes increasingly more important. This observation suggests that, to accurately model and generate extreme events using score-based models, incorporating the adjustment step is essential.

Generalized Extreme Value (GEV) Distribution The Generalized Extreme Value (GEV) distribution is commonly used to model the maxima of datasets and is defined by its probability density function (PDF):

$$f(x; \xi, \mu, \sigma) = \begin{cases} \frac{1}{\sigma} (1 + \xi \frac{x-\mu}{\sigma})^{-1-\frac{1}{\xi}} \exp\left(- (1 + \xi \frac{x-\mu}{\sigma})^{-\frac{1}{\xi}}\right), & \text{if } \xi \neq 0, \\ \frac{1}{\sigma} \exp\left(-\frac{x-\mu}{\sigma}\right) \exp\left(-\exp\left(-\frac{x-\mu}{\sigma}\right)\right), & \text{if } \xi = 0, \end{cases}$$

where: μ is the location parameter, $\sigma > 0$ is the scale parameter, ξ is the shape parameter (controls the tail heaviness).

The GEV distribution unifies three types of distributions: Gumbel ($\xi = 0$), Fréchet ($\xi > 0$), and Weibull ($\xi < 0$), making it highly flexible for extreme value analysis.

For the Fréchet distribution, moments of order k exist only if $k < \frac{1}{\xi}$. If $k \geq \frac{1}{\xi}$, the moment diverges, leading to infinite values. This property makes the Fréchet distribution particularly suited for modeling heavy-tailed distributions, as it captures the behavior of distributions with heavy tails and undefined higher-order moments.

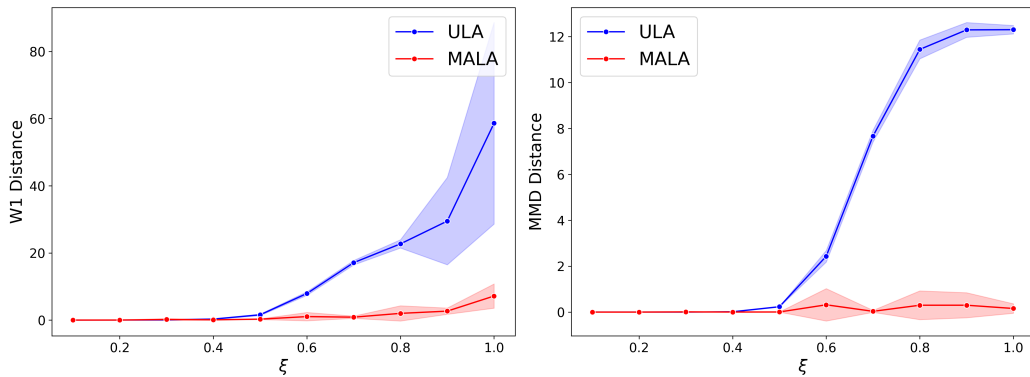
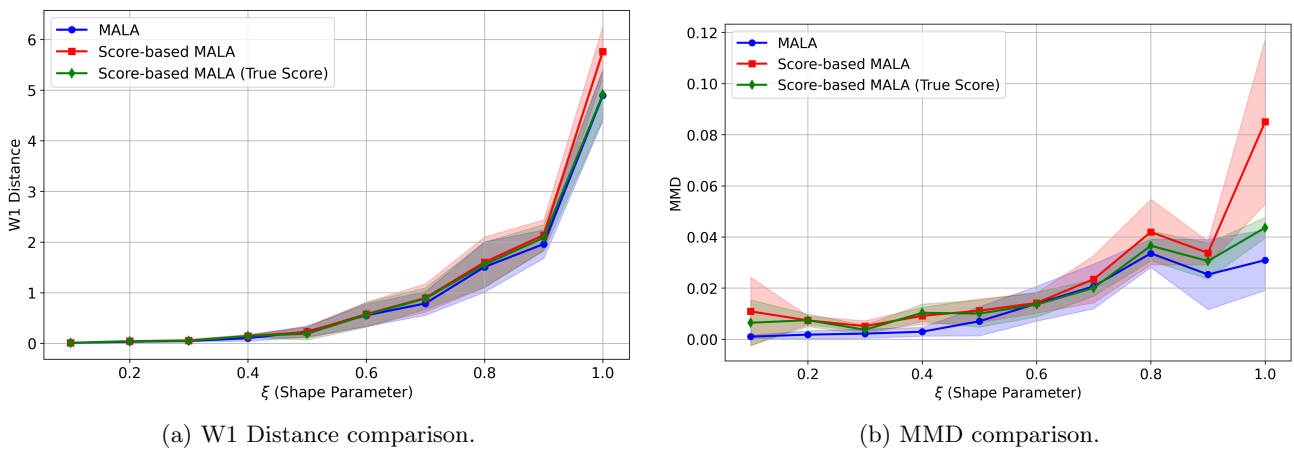


Figure 12: Comparison between ULA and MALA sampling methods for $GEV(0, 1, \xi)$, highlighting the effect of the adjustment step on heavy-tailed distributions. We fix the step size of both ULA and MALA to 0.1.

In Figure13, we illustrate that score-based MALA achieves competitive performance compared to the ground truth MALA. While MALA uses the standard acceptance function defined in Equation 1, score-based MALA learns a potentially different acceptance function.



(a) W1 Distance comparison.

(b) MMD comparison.

Figure 13: Comparison between score-based MALA (the score network is trained from data), score-based MALA (True Score) where the acceptance network is trained with the true score function, and the original MALA algorithm. Left: W1 distance. Right: MMD.

C Proofs

Proof of Proposition 1. Let $x, x' \in \mathcal{X}$. Suppose that the gradients on both sides are equal, i.e.,

$$\nabla \log a(x', x) - \nabla \log a(x, x') = \nabla \log p(x') - \nabla \log p(x) + \nabla \log q(x | x') - \nabla \log q(x' | x),$$

then integrating this equality gives:

$$\log a(x', x) - \log a(x, x') = \log p(x') - \log p(x) + \log q(x | x') - \log q(x' | x) + C,$$

where $C \in \mathbb{R}$ is a constant. Therefore, the acceptance function $a(x, x')$ can be expressed as:

$$\frac{a(x', x)}{a(x, x')} = e^C \cdot \frac{p(x')q(x | x')}{p(x)q(x' | x)}.$$

as e^C does not depend on x , setting $x = x'$, we get that

$$1 = e^C$$

Therefore we have that $C = 0$, which concludes the proof. □

Proof of Proposition 2. To prove that the acceptance function $a_M(x, x')$ satisfies the detailed balance condition, we need to show that:

$$p(x)q(x' | x)a_M(x', x) = p(x')q(x | x')a_M(x, x').$$

Substituting the definition of the acceptance function a_M , we consider two cases based on the value of the expression $\frac{p(x')q(x|x')}{p(x)q(x'|x)}$. Without loss of generality we consider the case when $\frac{p(x')q(x|x')}{p(x)q(x'|x)} \leq 1$, then by definition:

$$a_M(x', x) = \frac{1}{M} \frac{p(x')q(x | x')}{p(x)q(x' | x)}.$$

Substituting this into the detailed balance equation, we have:

$$p(x)q(x' | x) \cdot \frac{1}{M} \frac{p(x')q(x | x')}{p(x)q(x' | x)} = \frac{1}{M} p(x')q(x | x').$$

Similarly, since $\frac{p(x)q(x'|x)}{p(x')q(x|x')} \leq 1$ in this case, we have:

$$a_M(x, x') = \frac{1}{M}.$$

Thus, the right-hand side of the detailed balance condition becomes:

$$\frac{1}{M} p(x')q(x | x')$$

Therefore, both sides are equal:

$$\frac{1}{M} p(x')q(x | x') = \frac{1}{M} p(x')q(x | x'),$$

which confirms that the detailed balance condition holds in this case. □

D Experiments Details

In this section, we provide descriptions of the datasets used to generate the empirical results from the main text, and outline the neural network architectures and hyperparameter choices. All presented empirical results were compiled using an NVIDIA RTX 3090 GPU.

D.1 Dataset Descriptions

We use four datasets generated using `scikit-learn` (Pedregosa et al., 2011) and custom code. The parameters provided ensure reproducibility of the results:

- **Moons:** This dataset consists of two interlocking crescent-shaped clusters. We generate 10000 samples with a noise level of 0.1 using `sklearn.datasets.make_moons(n_samples=10000, noise=0.1)`.
- **Pinwheel:** Data points are arranged in six spiral arms. We generate 10000 samples with a radial standard deviation of 0.5, tangential standard deviation of 0.05, and a rate of 0.25 (which controls the spread of the arms). The dataset is generated using custom code and the following parameters:
 - `num_classes=5`,
 - `radial_std=0.5`,
 - `tangential_std=0.05`,
 - `rate=0.25`.

Algorithm 3 Pinwheel Dataset Generation

- 1: **Input:** Number of samples n , number of classes K , radial standard deviation σ_r , tangential standard deviation σ_t , rotation rate α
- 2: **Output:** Dataset $\mathbf{X} \in \mathbb{R}^{n \times 2}$
- 3: Generate random class labels $\mathbf{y} \in \{0, 1, \dots, K-1\}$ for n samples
- 4: Compute angles $\theta_k = \frac{2\pi k}{K}$ for each class $k \in \{0, 1, \dots, K-1\}$
- 5: Generate radial components $r_i \sim \mathcal{N}(1, \sigma_r^2)$ for each sample i
- 6: Compute tangential noise $\delta_i \sim \mathcal{N}(0, \sigma_t^2)$ for each sample i
- 7: Compute angle for each point: $\phi_i = \theta_{y_i} + \alpha \cdot r_i$
- 8: Compute Cartesian coordinates:

$$x_i = r_i \cdot \cos(\phi_i) + \delta_i$$

$$y_i = r_i \cdot \sin(\phi_i) + \delta_i$$

- 9: Return the dataset $\mathbf{X} = \{(x_i, y_i)\}_{i=1}^n$
-

- **S-curve:** This dataset consists of 10000 points distributed along an "S"-shaped 3D manifold with added Gaussian noise of 0.1. It is generated using `sklearn.datasets.make_s_curve(n_samples=10000, noise=0.1)`.
- **Swiss Roll:** This dataset contains 10000 points arranged along a 3D spiral-shaped surface, with Gaussian noise of 0.5 added. It is generated using `sklearn.datasets.make_swiss_roll(n_samples=10000, noise=0.5)`.

All datasets are converted to PyTorch tensors for further processing. The experiments were performed using an NVIDIA RTX 3090 GPU.

D.2 Neural Network Architectures

We now provide detailed descriptions of several different neural network architectures designed for learning the score function (Score Nets), and the acceptance networks (Acceptance Nets).

Score Nets. The Score Nets architecture is a simple feed-forward neural network consisting of an input layer, two hidden layers, and an output layer. The input dimension is the same as the output dimension, ensuring that the output matches the shape of the input data. The `Softplus` activation function is applied after each hidden layer to introduce non-linear transformations. The output layer does not use an activation function, as it directly produces the estimated score of the input.

Acceptance Nets. The Acceptance Nets architecture is a feed-forward neural network designed to compute the acceptance function for a pair of inputs. The network takes two input vectors, concatenates them, and passes the result through an initial fully connected layer with a customized hidden dimension. Following this, the network consists of three residual blocks, each containing fully connected layers with the same hidden dimension, enhanced by GELU activation functions to improve non-linearity and gradient flow. Finally, the output is passed through a fully connected layer, followed by GELU and a Sigmoid activation to ensure the output is between 0 and 1, representing the acceptance probability.

D.3 Hyperparameters

Score Nets. We summarize the hyperparameters used to train the Score Nets in Table 2.

Table 2: Score-Net Training Hyperparameters

Dataset	Optimizer	Learning Rate (LR)	Epochs	Hidden Dimension
Moons	Adam	1×10^{-3}	5000	64
Pinwheel	Adam	5×10^{-4}	2000	512
S-curve	Adam	5×10^{-4}	2000	512
Swiss Roll	Adam	5×10^{-4}	2000	512

Acceptance Nets. We provide below the detailed for training the Acceptance network for the various score-based Metropolis-Hastings algorithms.

Table 3: Acceptance-Net Training Hyperparameters

Dataset	Optimizer	LR	Hidden Dimension	Residual Layers	Epochs	λ
Moons	Adam	5×10^{-4}	256	3	1000	2
Pinwheel	Adam	5×10^{-4}	256	4	200	2
S-curve	Adam	5×10^{-4}	512	4	200	2
Swiss Roll	Adam	5×10^{-4}	512	4	200	1